ELSEVIER

Contents lists available at ScienceDirect

Journal of Cleaner Production

journal homepage: www.elsevier.com/locate/jclepro





Machine learning-enhanced uncertainty quantification for renewable-powered hybrid green ammonia and refrigeration systems: Technoeconomic and environmental effects

Muzumil Anwar^{a,*}, Israfil Soyler^a, Nader Karimi^{b,**}

- ^a School of Engineering and Materials Science, Queen Mary University of London, London, E1 4NS, United Kingdom
- ^b School of Engineering, University of Southampton, Southampton, SO16 7QF, United Kingdom

HIGHLIGHTS

- ML-enhanced UQ approach cuts computational cost while ensuring high accuracy.
- Analysis shows 18 % NH3 production and 30 % refrigeration output variability.
- Heat exchanger effectiveness drives 50 % of system uncertainty.
- System uncertainties cause 40–50 % variation in CO₂ reduction potential.
- Economic impact: 30-40 % refrigeration revenue and 5 % LCOA fluctuation.

ARTICLE INFO

Keywords: Uncertainty quantification Machine learning Techno-economics Green ammonia production Waste heat recovery Hybridised energy systems

ABSTRACT

Renewable-powered ammonia production is a promising route for sustainable energy and hydrogen storage but is highly sensitive to operational uncertainty from variable power supply and component performance. This study presents a novel machine learning-enhanced uncertainty quantification (ML-UQ) framework that, for the first time, integrates a high-fidelity surrogate model—an artificial neural network with autoregressive feedback—into Aspen Plus simulations of a hybrid ammonia production system coupled with a vapour absorption refrigeration unit for heat recovery. The framework captures nonlinear interactions among six critical uncertain parameters, including renewable power variability, heat exchanger effectiveness, and compressor efficiency. It reduces the computational cost by three orders of magnitude while maintaining high predictive accuracy (R² = 0.97, MAE = 8.57, RMSE = 11.3). The ANN surrogate enables scalable uncertainty propagation via polynomial chaos expansion. Results show that, across nominal power levels of 10-20 MW, uncertainties can cause up to 18 % variation in ammonia output, 30 % in refrigeration, and 40-50 % in CO2 emissions reduction. Heat exchanger effectiveness alone accounts for nearly 50 % of total variability. Economic analysis indicates a 5 % increase in the levelized cost of ammonia and 30-40 % variation in annual refrigeration revenue. This work delivers the first computationally feasible, ML-assisted surrogate-based UQ framework for hybrid green ammonia systems. More broadly, it offers a practical and readily scalable tool for designing resilient, economically viable, and low-carbon energy and chemical manufacturing systems.

Nomenclature:		(continued)	
		b^l	Bias vector
AWE	Alkaline water electrolyser	$C_{ m eff}$	Compressor's isentropic efficiency
σ^l	Activation function elementwise	C_k	PCE coefficients
ASU	Air separation unit	CPU	Central processing unit
	(continued on next colum	n)	(continued on next page)

^{*} Corresponding author.

E-mail addresses: muzumil.anwar@qmul.ac.uk (M. Anwar), Nader.Karimi@soton.ac.uk (N. Karimi).

https://doi.org/10.1016/j.jclepro.2025.146702

^{**} Corresponding author.

(continued)

CoV	Coefficient of variation
d	Dimension
GHG	Greenhouse gasses
HB	Haber Bosch
HPC	High performance computer cluster
λ	Simulation outputs
ξ	Quadrature points
LCOA	Levelized cost of ammonia
N	Number of PCE terms
Nord	Parameter used for quadrature point generation
P	Order of PCE model
PCE	Polynomial chaos expansion
PDF	Probability density function
P _{sample}	Sample parameters
S	Main sensitivity
SD	Standard deviation
UQ	Uncertainty quantification
UQTk	Uncertainty quantification tool kit
VARC	Vapour absorption refrigeration cycle
W^l	Weight matrix
$\Psi_{\mathbf{k}}$	Multidimensional orthogonal polynomials
WHR	Waste heat recovery
x	Uncertain parameter
$\widehat{\mathbf{y}}$	Outputs
π	Probability density function (PDF)

1. Introduction

1.1. Background

The increasing utilisation of renewable power sources, particularly wind and solar photovoltaic, presents challenges due to their inherent variability and intermittency, thereby necessitating efficient and scalable energy storage solutions (Almodfer et al., 2022; Y. Wang et al., 2024). Among the various energy carriers, hydrogen has emerged as a promising long-term option, particularly in its green form-produced via water electrolysis powered by renewable energy (Samitha Weerakoon and Assadi, 2024), the practical deployment of hydrogen is constrained by high storage costs, energy-intensive liquefaction processes, and transportation safety concerns (T. Zhang et al., 2023). In this context, ammonia is gaining recognition as an alternative hydrogen carrier, owing to its higher volumetric energy density, ease of storage under moderate pressure and temperature, and existing global infrastructure for handling and distribution (Díaz-Motta et al., 2023; Xing and Jiang, 2024). Despite these advantages, ammonia synthesis is highly sensitive to fluctuations in renewable power supply, leading to operational uncertainties that challenge the economic viability (Rehman et al., 2024; Verleysen et al., 2020). However, systematic, and cost-effective evaluation of these uncertainties remains unexplored and calls for further research.

1.2. Literature review

1.2.1. Green ammonia production

Recent advancements have focused on decarbonising ammonia production through the integration of renewable energy sources, enhancing both economic viability and sustainability. For instance, Shamsi et al. (2024) demonstrated a geothermal-powered polygeneration system that integrates a PEM electrolyser, an organic Rankine cycle, and an air separation unit, co-producing ammonia, electricity, oxygen, and thermal energy. This configuration achieved an ammonia output of 2.085 kg/s at a competitive cost of \$2.24/kg with a payback period of just three years, underscoring the feasibility of geothermal-based synthesis. Electrolyser selection has also proven critical; Nami et al. (2024) compared alkaline (AEC) and solid oxide (SOEC) electrolysers, revealing that while AEC is cost-effective today, SOEC's higher efficiency and thermal integration capabilities could reduce production costs to $340 \ \epsilon/t$ with low-cost electricity ($10 \ \epsilon/MWh$), making it competitive with

fossil-based ammonia. To further expand renewable integration, decentralised ammonia production systems leveraging biomass gasification, biogas reforming, and electrolysis have been modelled in Aspen Plus, maintaining consistent primary energy consumption (~14-15 kW/kg NH₃) without compromising process efficiency (Frattini et al., 2016). To further optimise energy and exergy efficiencies, a recent study (Anwar et al., 2024) conducted 4 E analysis (energy, exergy environment and economy) and compared waste heat recovery methods in green ammonia plants. It was found that the vapour absorption refrigeration cycle significantly outperforms the Kalina cycle by enhancing energy efficiency by 8 %, improving exergy efficiency by 11 %, and quadrupling emission savings, all while maintaining cost-effectiveness. Beyond traditional methods, emerging low-pressure synthesis techniques-including thermochemical looping, solid-state synthesis, and photocatalysis—seek to bypass the energy-intensive Haber-Bosch process. These methods promise reduced energy demand and enhanced integration with variable renewable sources (Klaas et al., 2021). Additionally, Laimon and Goh, 2024 introduced a framework to repurpose curtailed renewable electricity for ammonia synthesis, incorporating capacity factor adjustments and monetising by-products, achieving levelized costs of \$1.5/kg for hydrogen and \$401/t for ammonia. This strategy not only improves economic feasibility but also enhances grid stability by utilising surplus renewable energy. While the economics and efficiency of green ammonia production have been widely studied, the impacts of uncertainties on economic outcomes and plant performance remain largely unexplored.

Machine Learning (ML) has further accelerated innovation in green ammonia production, enabling efficient processing of high-dimensional data, optimising plant performance, and supporting real-time decisionmaking (Sarker, 2021; Zaki et al., 2024; Zhang and Jiang, 2018). ML-driven models have been instrumental in predicting energy consumption, detecting inefficiencies, and suggesting corrective strategies that lead to cost savings and emission reductions (El-Maghraby et al., 2024; Qaiyum et al., 2025). Advanced optimisation frameworks and hybrid systems—such as geothermal-biomass co-production—have demonstrated improved ammonia yields and reduced environmental footprints (Yin, 2024; Zayed et al., 2025). Moreover, deep learning and physics-informed modelling have shown strong potential in optimising reactor configurations and understanding reaction kinetics, offering scalable solutions for process enhancement (Deng et al., 2024; Park et al., 2025). These technological advancements highlight the critical role of artificial intelligence in elevating technoeconomic analysis, emissions estimation, and system-wide optimisation within green ammonia production (Adeli et al., 2024; Lee et al., 2024). However, the consideration of uncertainties in machine learning-enhanced analyses is still rare.

1.2.2. Applications of uncertainty quantification to energy and production systems

Uncertainty Quantification is a critical framework for assessing the reliability and resilience of energy systems under variable conditions (Smith, 2024). It systematically measures uncertainties in system inputs and outputs, classifying them as either aleatoric (inherent variability) or epistemic (knowledge-based uncertainty) (Abdar et al., 2021; Helton et al., 2010; Wang, 2019). While aleatoric uncertainties are irreducible due to their stochastic nature, epistemic uncertainties can be reduced through improved data collection (Gholaminezhad et al., 2016). Accurate UQ enables robust performance predictions, which are vital for decision-making in complex production systems Nannapaneni and Mahadevan (2014); Zayed et al. (2023) applied a hybrid framework combining support vector machines and Monte Carlo simulation to assess how geometric and thermal parameters affect the performance of a wavy corrugated solar air collector with thermal energy storage. Their sensitivity analysis of key inputs demonstrated the effectiveness of data-driven modelling in renewable thermal energy systems. Traditional UQ methods, such as Monte Carlo simulations, are reliable but

computationally expensive, making them impractical for large-scale systems (Knio et al., 2001). To overcome this limitation, surrogate models like Gaussian Processes (Bilionis and Zabaras, 2012; Tripathy et al., 2016) and PCE (Najm, 2009; Zhang and Jiang, 2018) have been developed. PCE, initially introduced by Wiener and later refined (Egolfopoulos et al., 2014), is particularly effective—it reduces computational costs while maintaining accuracy in uncertainty propagation, making it ideal for analysing variability in energy and manufacturing systems.

Despite its importance, UQ is still underexplored in renewablepowered ammonia production. Few studies have examined how renewable supply fluctuations, process inefficiencies, and equipment variability affect outputs in hybrid ammonia systems. Extending UQ beyond ammonia synthesis to wider energy and manufacturing contexts is essential for robust, data-driven decision-making. As UQ advances, its integration into process modelling will be pivotal for improving predictive reliability and ensuring the long-term viability of sustainable production systems. However, the high computational cost of such analyses has slowed down the progress on this front. The integration of machine learning surrogates for real-time predictions remains an outstanding challenge, emphasising the need for more scalable, highfidelity UQ approaches in multi-scale energy and production systems. For example, Soyler et al. (2023) showed that PCE can be an efficient alternative to Monte Carlo for assessing fuel composition effects in ammonia-hydrogen flames. However, even using a one-dimensional model, their uncertainty analysis of the basic combustion characteristics still required 6000 CPU hours. In a subsequent study, Soyler et al. (2024) extended the method to NH₃/syngas combustion, requiring 1296 samples per simulation—underscoring the persistent computational challenges in surrogate-based UQ.

1.3. Objectives and novelties

The primary objective of this work is to develop a robust methodology for quantifying the effects of uncertainties from multiple sources on the performance of ammonia production systems, and ultimately on their economic and environmental outcomes. To this end, we apply UQ to a hybrid ammonia production system, where performance is affected by uncertainties in heat exchangers, compressors, and renewable power supply. As process models become increasingly complex, traditional UQ methods are computationally prohibitive. To overcome this challenge, we introduce a novel machine learning-enhanced UQ framework that integrates an artificial neural network (ANN) surrogate model with Aspen Plus simulations. The ANN is coupled with the Uncertainty Quantification Toolkit (UQTk) to enable efficient uncertainty propagation, dramatically reducing computational cost while maintaining accuracy. This framework allows extensive analysis of uncertainties in ammonia production, refrigeration generation, GHG emissions reduction, and revenue-tasks that would otherwise be intractable using conventional methods.

The key novelty of this work lies in its seamless integration of ML within the UQ framework, enabling scalable and efficient uncertainty quantification for hybridised ammonia production. To the best of our knowledge, this study presents the first uncertainty quantification analysis of such hybrid ammonia-refrigeration systems and is among the earliest to apply machine learning techniques to ammonia production more broadly. By replacing exhaustive simulations with an ML-based surrogate model, our approach achieves remarkably high computational efficiency without compromising accuracy, making high-fidelity UQ feasible for complex, real-world energy systems.

2. Methodology

2.1. System description

Our previous study showed that integrating a green ammonia plant

with a vapour absorption refrigeration cycle significantly improves energy and exergy efficiencies while ensuring economic viability and substantial $\rm CO_2$ reduction (Anwar et al., 2024). However, that analysis did not consider operational uncertainties. Here, we examine six key uncertain parameters: heat exchanger effectiveness (HE1–HE4), compressor isentropic efficiency, and electrolyser input power, chosen for their strong influence on ammonia synthesis and thermal integration (Rajeh et al., 2024). Heat exchanger effectiveness can vary up to 20 % due to fouling and degradation (Karimi Shoar et al., 2023; Palmer et al., 2016; Zubair et al., 2000), compressor efficiency fluctuates by ~ 6 % (Gresh, 2018; Jain et al., 2013; Lou et al., 2013), and electrolyser power, from intermittent renewables, can change by up to 10 % (Lee et al., 2017; Suberu et al., 2014; Verleysen et al., 2020).

The schematic diagram shown in Fig. 1 represents the integrated system combining a power to hydrogen unit with Haber-Bosch (HB) process and waste heat recovery (WHR) i.e. vapour absorption refrigeration cycle (VARC). The power to hydrogen and HB sub-systems utilises air, water, and renewable power as inputs, producing green ammonia as the primary output and generating waste thermal energy as a byproduct. It is assumed that the renewable power input undergoes gradual, non-abrupt fluctuations, allowing the system to be modelled under quasi-steady-state conditions for the purpose of uncertainty quantification. This waste heat is effectively harnessed by VARC for refrigeration production, thus forming a hybridised ammonia synthesis plant. The refrigeration output from VARC represents a low carbon energy vector with significant economic value (Anwar et al., 2024).

2.2. Aspen Plus model

Aspen Plus V11 was used to conduct process simulations. A detailed illustration of Aspen Plus simulation models of the hybridised ammonia production system, incorporating an alkaline water electrolyser (AWE), air separation unit (ASU), and VARC, is shown in Fig. 2. In this system, nitrogen was produced through the ASU, hydrogen was generated via AWE. During electrolysis, water was decomposed in the electrolyser, producing hydrogen and oxygen. The resulting hydrogen and nitrogen streams were then supplied to the HB sub-system for ammonia synthesis. The VARC was integrated with HB through waste heat streams, specifically high-temperature (HT) and low-temperature (LT) streams labelled HB2-HT and HB2-LT, respectively. To maximise the utilisation of waste heat, a pre-heating system was introduced. This mechanism utilised hot outlet streams from the electrolyser, including oxygen streams (O2-HT, O2-LT) and hydrogen streams (H2-HT, H2-LT). Additionally, a third preheater was also used to extract heat from the stream HB streams (HB1-HT, HB1-LT), that hot stream was located preceding to the ammonia reactor in HB sub-system. This arrangement enhanced thermal efficiency and optimised the recovery of waste heat for the integrated WHR applications (Anwar et al., 2024). It is important to note here that the hybridised ammonia production model in Aspen Plus was validated extensively in our previous work (Anwar et al., 2024). Therefore, the validation is not repeated here.

Fig. 3 displays the Aspen Plus process models developed for the hybrid ammonia production system. The system components include: (1) a cryogenic air separation unit for nitrogen generation (Fig. 3a), (2) an alkaline water electrolyser for hydrogen production (Fig. 3b) modelled following Sanchez et al. (2020) with validated performance, and (3) a Haber-Bosch synthesis loop where ammonia is produced under high-pressure, high-temperature conditions (Fig. 3c), with model validation against Ishaq and Dincer (2020) data. For enhanced efficiency through waste heat recovery, the Haber-Bosch process was thermally integrated with a VARC. This integration was achieved using two high-temperature waste heat streams: HB1-HT (upstream of the HB reactor) and HB2-HT (outlet of high-pressure compressors), which serve as heat sources for the VARC system through dedicated heat exchangers. This configuration ensures continuous heat supply while maintaining energy balance across the hybrid system.

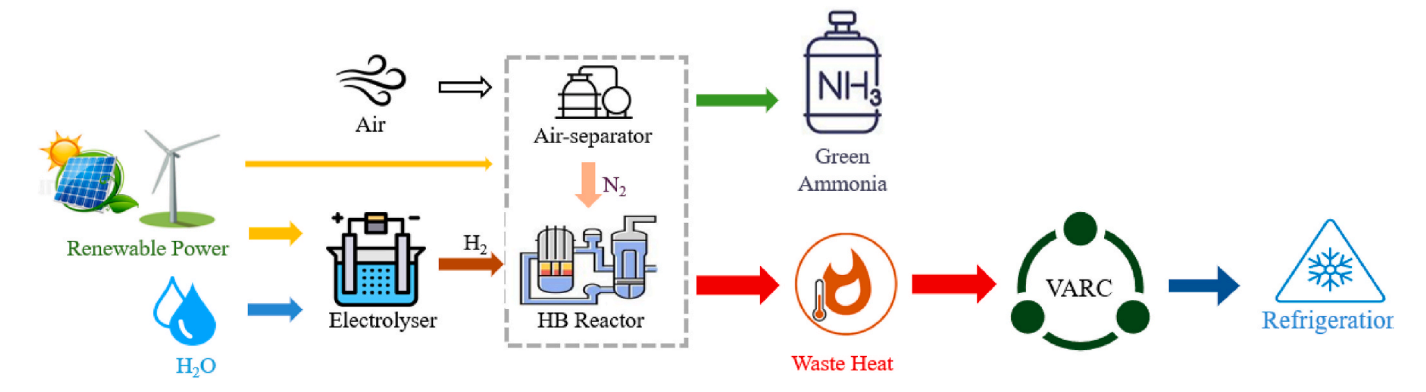


Fig. 1. Schematic of the investigated power to hydrogen and HB sub-system integrated with VARC, forming the hybridised ammonia production system.

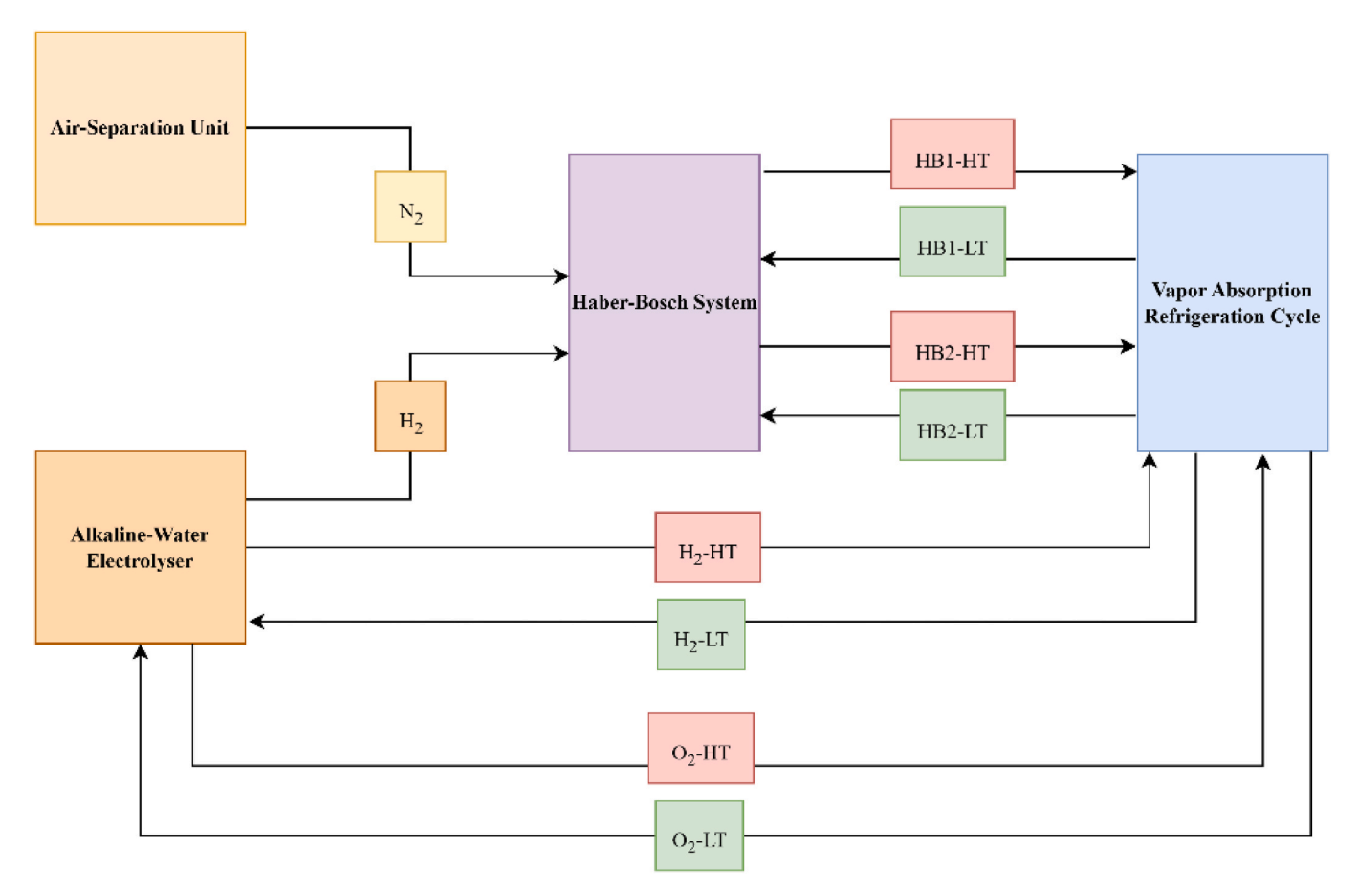


Fig. 2. Aspen plus model illustration of the hybridised ammonia production system.

2.3. Machine learning

The study employed a NARX-configured feedforward ANN with autoregressive feedback to model the integrated ammonia production system. This architecture combines feedforward ANN's nonlinear approximation capability with temporal memory through input/output delays, effectively capturing system dynamics and uncertainty propagation. As shown in Fig. 4, the network comprises an input layer, fifteen fully connected hidden layers using tansig activation functions, and a linear output layer (purelin) for continuous regression. Input and feedback delays (1–2 timesteps) were incorporated to account for historical trends in key parameters (renewable power, heat exchanger effectiveness, compressor efficiency) and outputs (ammonia production, refrigeration). The network was first trained in open-loop mode before

conversion to closed-loop for multi-step forecasting. A step-ahead prediction variant was also developed by reducing one delay, enabling proactive system control through single-timestep anticipation.

The hyperparameter tuning process proceeded in two phases. Initial baseline configurations were established through empirical evaluation of delay lengths, hidden layer architecture, learning rates, epoch counts, and training functions. Subsequently, Bayesian optimisation refined key parameters—neuron count, learning rate, and regularisation strength—using a probabilistic surrogate model to minimise crossvalidated MSE while efficiently navigating the search space (Snoek et al., 2012; Z. Wang et al., 2024). This approach optimally balances exploration and exploitation, particularly valuable for computationally intensive model evaluations. The final model employed Levenberg-Marquardt backpropagation (Yang et al., 2021) for rapid

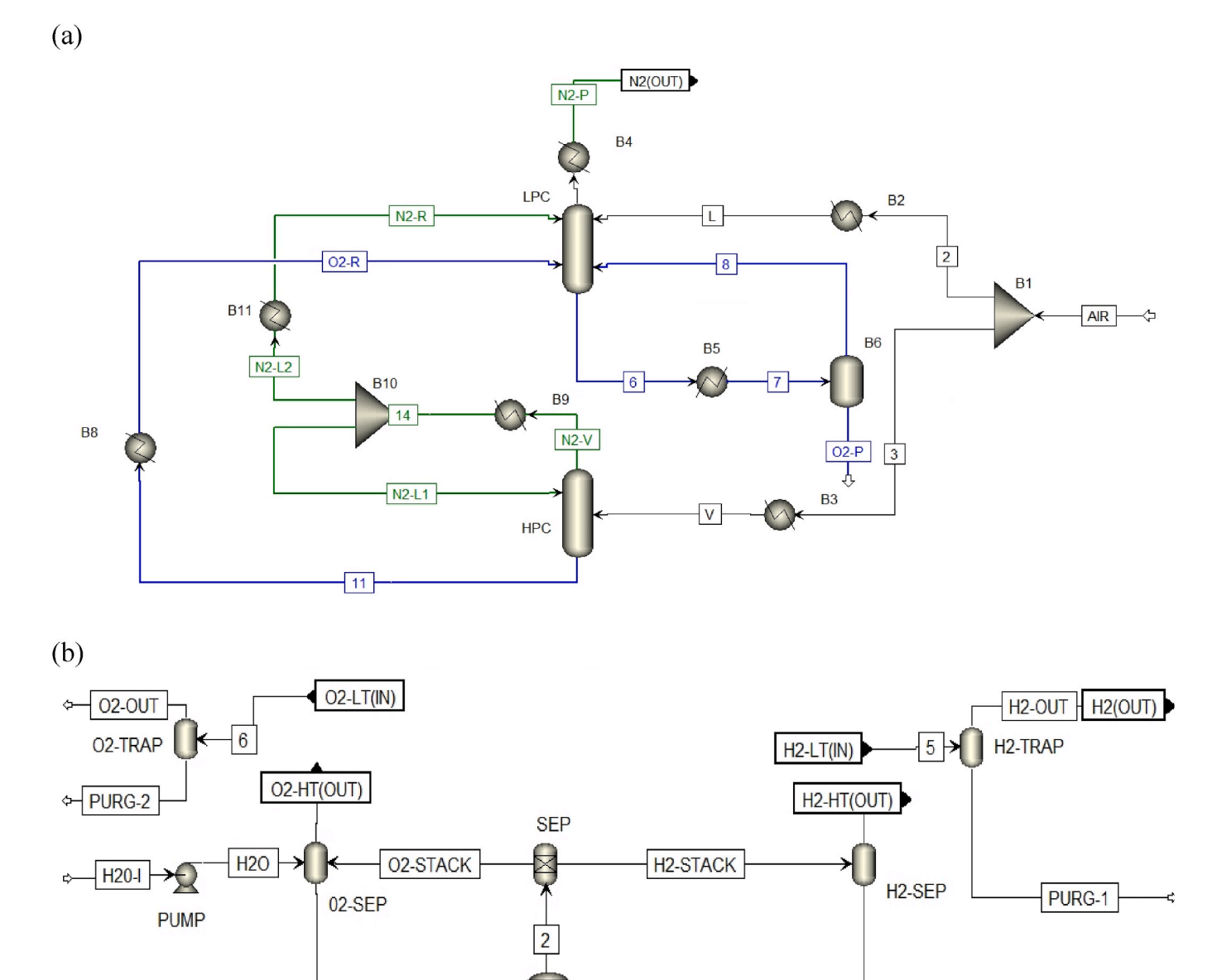


Fig. 3. Aspen Plus models of (a) ASU, (b) AWE, (c) HB sub-system, (d) VARC.

REACTOR

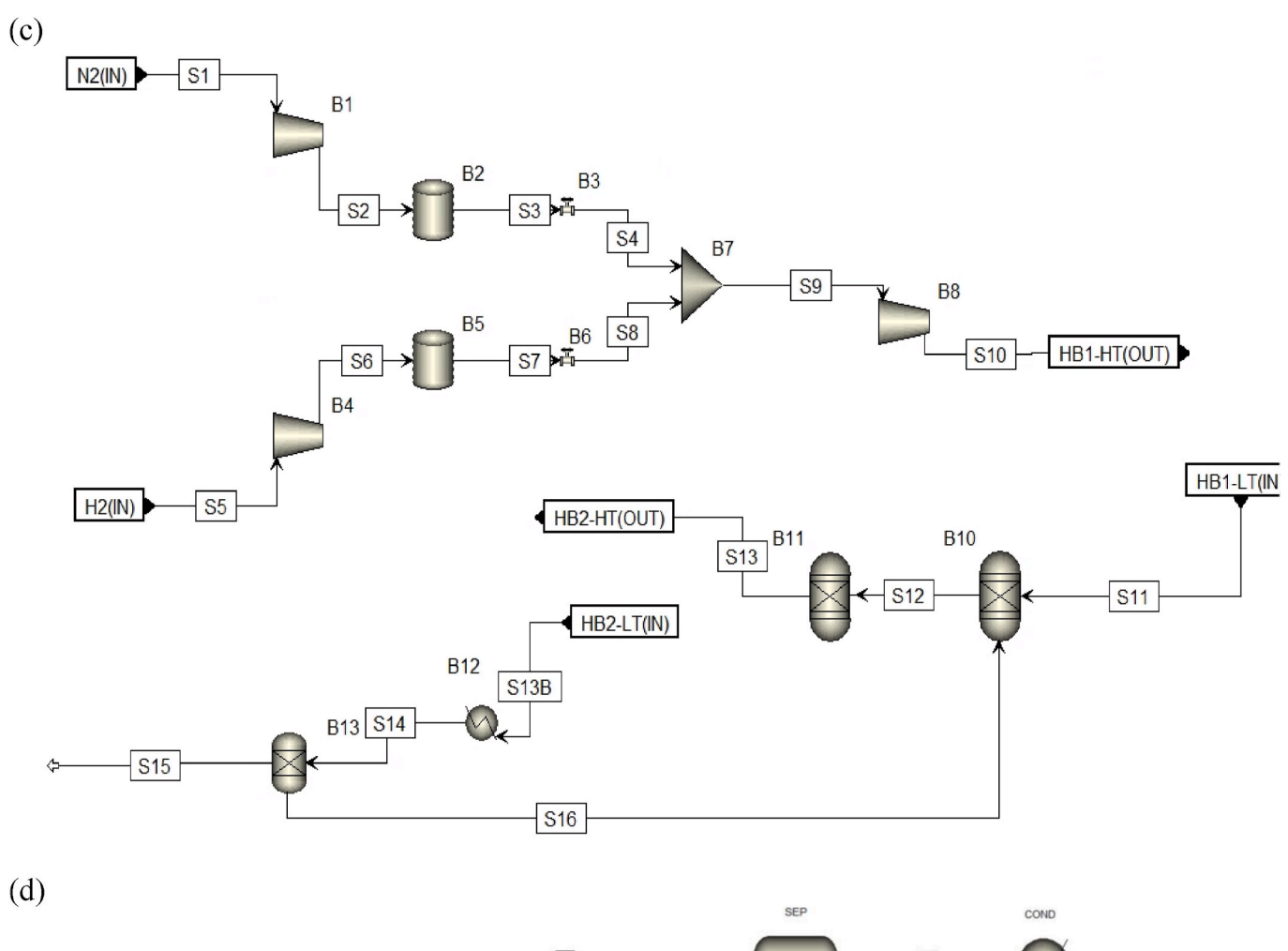
INLET

convergence, achieving excellent predictive performance ($R^2=0.967$, MAE = 8.57, RMSE = 11.3, Grayson Index = 0.98). Cross-validation with multiple input sets from the uncertainty quantification toolkit confirmed the model's robustness and generalisation capability. The surrogate demonstrated both computational efficiency and strong

O2-KOH

agreement with Aspen Plus simulations, as evidenced by probability density function analyses in Section 2.5.1. Once validated, the ML model was used to predict system behaviour across six configurations (10–20 MW power input), enabling comprehensive UQ analysis without the computational burden of extensive simulations. The final ANN

H2-KOH



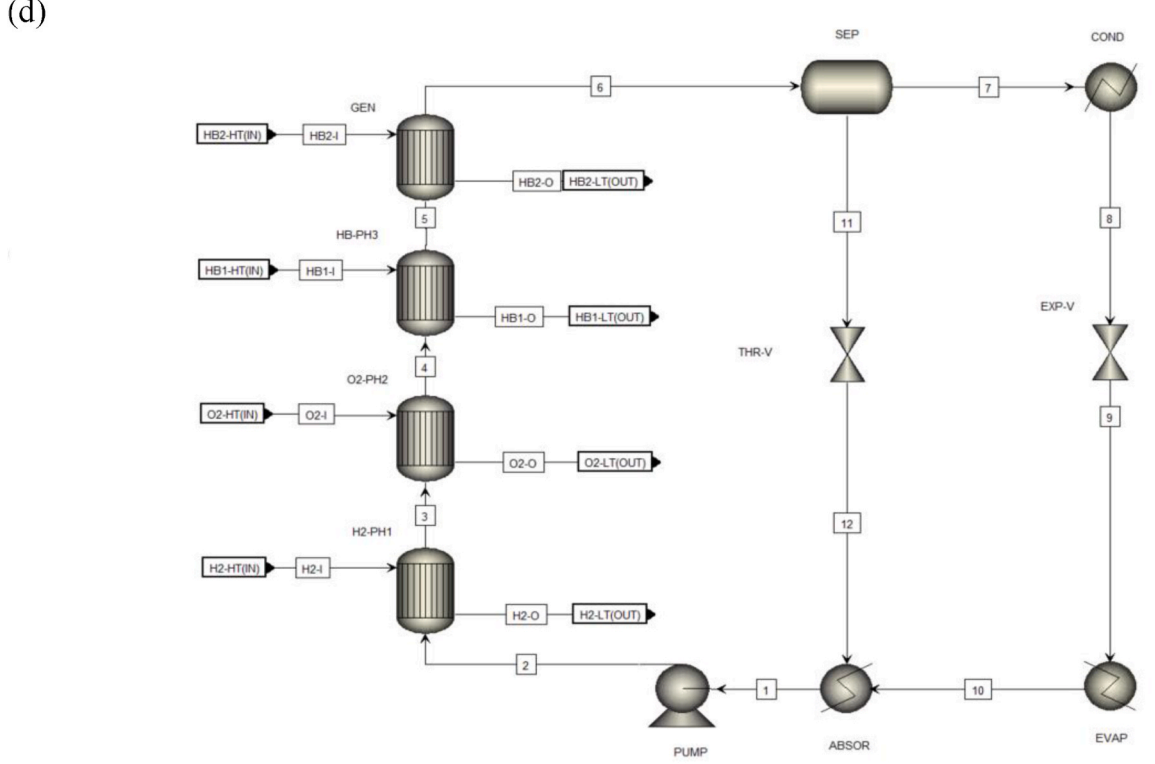


Fig. 3. (continued).

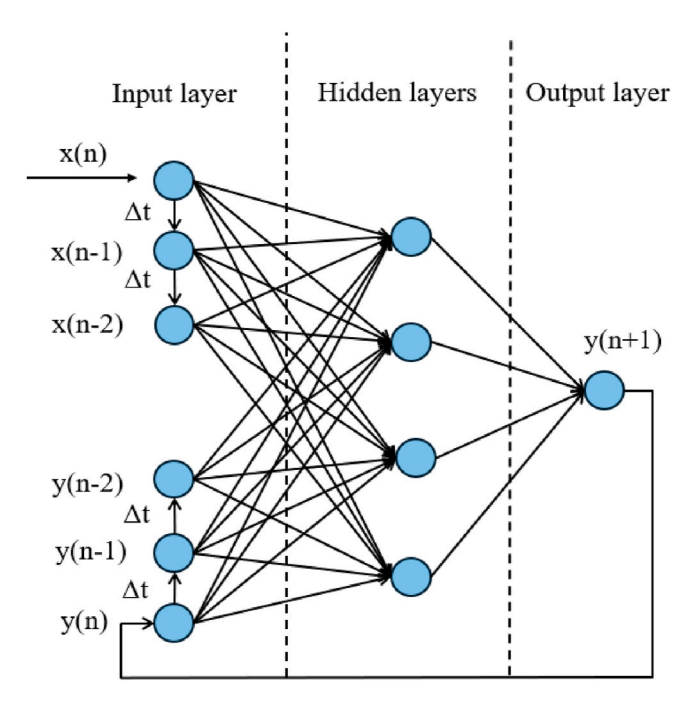


Fig. 4. Architecture of ML model.

predictive model is expressed as:

$$\widehat{y} = f_{ANN}(x) = \sigma^{l}(W^{l}\sigma^{l-1}(\dots \sigma^{l}(W^{1}x + b^{1})\dots) + b^{L})$$
(1)

As shown later, this approach significantly enhances computational efficiency while maintaining precision in UQ analysis.

2.4. Uncertainty quantification

In this study, an open-source UQTk, version 3.1.2 (Bert Debusschere, 2024; Sargsyan et al., 2022) was employed to construct PCE models and process the resulting data. UQTk works by running the model thousands of times with different input samples, allowing uncertainty to be propagated through system. A python script was developed to generate random parameter samples utilising the mean values which can be seen in Table 1.

The uncertainty in the simulation parameters is represented by Eq.

$$P_{sample} = P_{\mu} \pm P_{\sigma} * \xi_d \tag{2}$$

Here, P_{sample} represents one of the simulation parameters, where its uncertainty is randomly sampled. The mean value and standard deviation of the corresponding parameters are denoted as P_{μ} and is P_{σ} , respectively, that can be seen in Table 1.

In Equation (2), ξ_d represents the random variable components, referred to as dimensions, which can be expressed as $\xi_d = (\xi_{HE1}, \xi_{HE2}, \xi_{HE1}, \xi_{HE2}, \xi_{HE2}, \xi_{HE1}, \xi_{HE2}, \xi_{HE2}, \xi_{HE2}, \xi_{HE1}, \xi_{HE2}, \xi_{H$

Table 1 Mean values of uncertain parameters. 10

Nominal

12

power input (MW)								
Parameters (P)	Mean values							
HE1 (kW)	811.37	874.80	979.75	1030.55	1176.94	1313.47		
HE2 (kW)	63.12	77.13	91.13	101.72	115.91	126.22		
HE3 (kW)	28.53	33.72	38.48	41.76	45.69	48.31		
HE4 (kW)	675.84	710.21	765.11	814.68	878.02	913.66		
P _{in} (MW)	10	12	14	16	18	20		
C _{eff} (%)	75	75	75	75	75	75		

18

20

 $\xi_{HE3}, \xi_{HE4}, \xi_{P_{in}}, \xi_{C_{eff}}$ where d indicates the dimensionality. These random variables, referred to as quadrature points, are generated according to the distribution type associated with the orthogonal polynomial series.

Several orthogonal polynomial series from the Wiener-Askey scheme are available in UQTk, including Laguerre, Jacobi, Hermite, and Legendre polynomials (Xiu and Karniadakis, 2002). The choice of method for constructing PCE is inherently linked to the distribution type of the uncertain parameters, such as uniform, normal, or exponential. PCE has been widely recognised in the literature as a robust method for quantifying uncertainties in complex engineering systems, providing a computationally efficient means of capturing the statistical properties of model outputs (Le Maitre et al., 2002; Najm et al., 2009; Reagan et al., 2005). In this study, the uncertainties in system parameters were assumed to be uniformly distributed, reflecting bounded variability without a specific directional bias. Consequently, Legendre polynomials were selected, as they are well-suited for uniformly distributed random variables (Mueller et al., 2025; Sargsyan et al., 2022). This choice is consistent with the steady-state assumptions of the renewable energy inputs and aligns with prior studies demonstrating the applicability of Legendre-based PCE for systematic uncertainty propagation in energy systems (Gillcrist et al., 2024; Xiong et al., 2014). Each uncertain parameter is defined within the interval [-1,1], allowing for a mathematically structured and representative characterisation of variability across the input space.

Consequently, Eq. (3) represents the PCE of a simulation output (λ).

$$\lambda = \sum_{k=0}^{p} C_k \Psi_k(\xi_d) \tag{3}$$

Here, λ represents a simulation output (i.e. ammonia production and refrigeration generation from hybridised ammonia production system), P represents the order of the polynomial chaos expansion model, while $\Psi_k(\xi)$ denotes the multidimensional orthogonal polynomial chaos Legendre-Uniform basis functions. The coefficients C_k corresponds to the PCE coefficients.

In UQTk, the methods to perform quadrature integration are either the sparse tensor product method or full tensor product method. For full tensor product technique, the function must be integrate using the quadrature points (ξ_d) , and their number is determined by $(N_{ord})^d$, where $N_{\text{ord}} = P{+}1$ is the order of expansion. In this study, P was set to three, resulting in $(3+1)^6 = 4096$ is quadrature points used for the integration. It is crucial to highlight that in high-dimensional problems, this technique demands significantly more computational resources, leading to the issue known as the curse of dimensionality (Indyk and Motwani, 1998). Furthermore, growing the order of PCE beyond a certain threshold does not always improve the results.

For balance accuracy and computational efficiency, a third-order PCE analysis was chosen for this study. Increasing the order substantially amplifies the computational cost, as it scales the random sample numbers $(N_{ord})^6$, for instance, $6^6 = 46,656$.

The 4096 quadrature points in ξ are transformed into 4096 P_{sample} values using Eq. (1). These P_{sample} simulations then performed in Aspen Plus to compute outputs, ammonia production and refrigeration generation, across nominal power inputs of the hybridised ammonia production system.

To determine the coefficients C_k , the non-intrusive spectral projection method is employed, utilising Gauss-Legendre quadrature integration (Jansohn, 2013) as described in Eq. (4).

$$C_{k} = \frac{\langle \lambda(\xi) \Psi_{k}(\xi) \rangle}{\langle \Psi_{k}^{2}(\xi) \rangle} = \frac{1}{\langle \Psi_{k}^{2}(\xi) \rangle} \int_{-1}^{1} \lambda(\xi) \Psi_{k}(\xi) \pi(\xi) d(\xi) \ k = 0, ..., P$$
 (4)

where (ξ) denotes the germ samples and $\pi(\xi)$ represents the PDF for each input parameters mentioned in Table 1.

Global sensitivity analysis plays a crucial role in UQ as it identifies the parameters that most significantly impact the output (Kucherenko and Song, 2017). In this study, Sobol' indices, a widely used method for sensitivity analysis, were applied. Eq. (5) was used to compute the sensitivity index to measure the contribution of the variance of single parameter to the overall output variance.

$$S_d = \frac{1}{V|\lambda|} \sum \lambda_d^2 \langle \Psi_d^2 \rangle \tag{5}$$

Here, S_d denotes the sensitivity which is associated to the dimension (d) and corresponds to the number of uncertain parameters. $V[\lambda]$ represents the total variance. For example, the total variance of the outputs (i.e. NH₃ production and refrigeration generation) can be expressed as shown in Eq. (6).

$$V[NH_3 / ref] = \sum_{k>0} \lambda_k^2 \Psi_k^2 \tag{6}$$

The numerator in Eq. (5) can be further expressed as shown in Eq. (7). For this study, the dimensionality d = 6, the total order P = 3, and the number of PC terms is calculated as N = (d + P)!/(d!P!) = 84. The first term in Eq. (7) corresponds to the mean value without any deviation and is thus equal to zero.

$$Var(NH_3 / ref) = 0 + \lambda_1^2 \Psi_1^2 + \lambda_2^2 \Psi_1^2 + \lambda_3^2 \Psi_1^2 + \lambda_4^2 \Psi_2^2 + \lambda_5^2 \Psi_1^2 + \dots (84 \text{ terms})$$
(7)

2.5. Machine learning enhanced uncertainty quantification

The conventional UQ approach using Aspen Plus simulations required 4096 simulations per nominal power input, resulting in over 1050 CPU hours. Simulations were performed on a Dell XPS 17 9700 with an 11th Gen Intel Core i9-11900H CPU @ 2.50 GHz and 64 GB RAM. Extending this analysis across nominal power inputs from 10 MW to 20 MW—reflecting typical scales of modular green ammonia systems powered by intermittent renewable sources (Chitransh and Bindal, 2021; Yuen et al., 2010; Y. Zhang et al., 2023)—made exhaustive direct simulations computationally infeasible.

To overcome this limitation, we developed a novel machine learning–enhanced UQ framework by integrating an artificial neural network (ANN) surrogate with Aspen Plus simulations. This approach drastically reduces computational overhead while maintaining high predictive fidelity. Embedding the ANN within the UQ workflow

achieved a three-order-of-magnitude reduction in computational cost compared to direct simulation. For example, analysing six system capacities (10–20 MW) with conventional simulations would require over 24,000 full-process runs, totalling approximately 6300 CPU hours. In contrast, once trained, the ANN model completed the same uncertainty propagation in under 7 h on the same hardware. This efficiency becomes even more critical as system complexity increases. Moreover, the framework is simulation-agnostic and scalable, allowing integration with platforms such as ANSYS, Aspen Plus, COMSOL, or MATLAB/Simulink. Its main strength is enabling rigorous uncertainty analysis for complex, nonlinear, and tightly coupled energy systems that are otherwise intractable with conventional methods.

We focused on six critical uncertain parameters: four heat exchanger effectiveness values (HE1–HE4), compressor efficiency ($C_{\rm eff}$), and electrolyser power input ($P_{\rm in}$). Using UQTk, these parameters were systematically sampled to ensure comprehensive coverage of the input space. The sampled inputs were processed through Aspen Plus to generate outputs for ammonia production and refrigeration generation. Unlike traditional direct simulations, the ANN surrogate replaces Aspen Plus runs, as illustrated in Fig. 5. While ML-UQ approaches have been applied in other engineering domains, this represents one of the first implementations tailored to hybrid green ammonia systems, providing a scalable alternative for UQ in this emerging field.

The ANN model was trained on the Aspen Plus simulation data, with its parameters optimised to minimise prediction error. Once validated, the ML-based model performed the UQ analysis in place of the full simulation. This integration greatly reduced computational time and resource usage while efficiently predicting system outputs—ammonia production, refrigeration generation, GHG emission reduction, and revenue—across the parameter space. By replacing exhaustive simulations that would have been prohibitive for large-scale analyses, the ML surrogate enabled comprehensive uncertainty quantification. This approach not only streamlines the analysis process but also supports timely, resource-efficient decision-making, highlighting the substantial benefits of ML-enhanced UQ in complex energy systems.

2.5.1. ML model validation

The ML model was rigorously validated through multiple approaches, including R² evaluation, output distribution comparisons, and uncertainty quantification assessment. Through iterative dataset

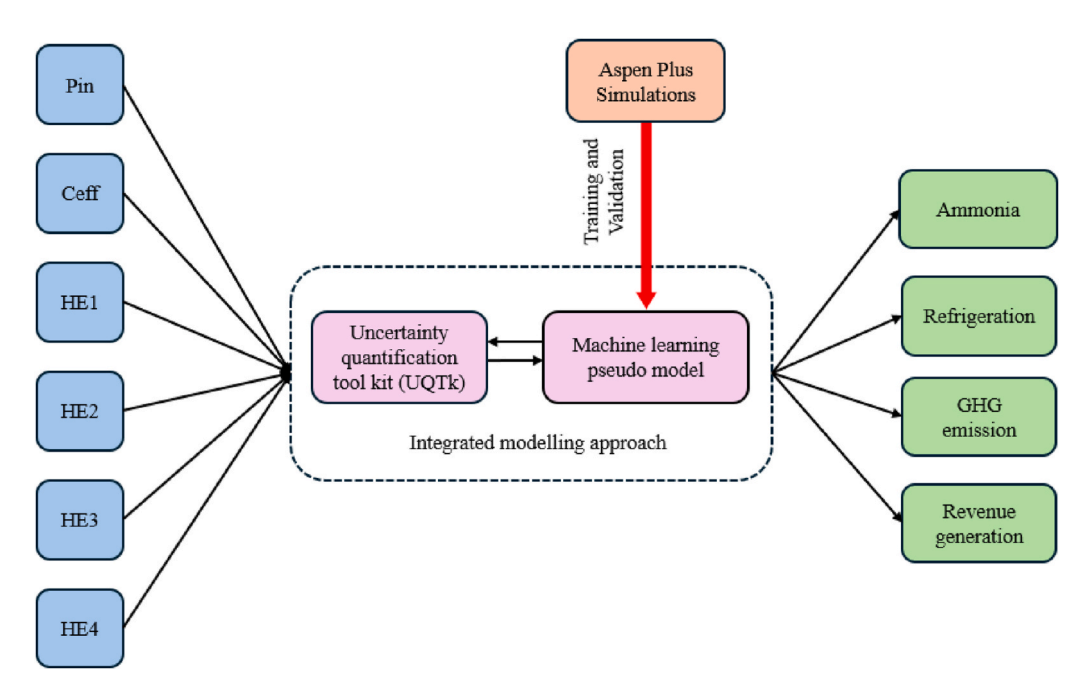


Fig. 5. Schematic representation of the novel 'ML enhanced UQ analysis' for the hybridised ammonia production system.

expansion, the model achieved strong predictive performance ($R^2=0.97$, MAE = 8.57, RMSE = 11.3), demonstrating excellent agreement with Aspen Plus simulations. Cross-validation using alternative UQTk-generated sample sets confirmed consistent performance across different data subsets, supporting framework reliability.

For model development, the dataset was progressively expanded and partitioned into 70 % training, 15 % validation, and 15 % test sets. Additional cross-validation using completely unseen "blind" data further verified the model's ability to accurately predict system behaviour under varying conditions. Fig. 6 compares probability density functions (PDFs) between Aspen Plus simulations and data-driven model results for both ammonia production and refrigeration generation. The ammonia production PDF shows a uniform distribution (Fig. 6a), reflecting linear variation propagation primarily influenced by input power and two heat exchangers. In contrast, refrigeration generation exhibits a normal distribution (Fig. 6b, bell-shaped curve), resulting from the combined effects of multiple interacting uncertainties (input power, several heat exchangers, compressor efficiency) following Central Limit Theorem principles (Davidson, 1994; Spanos, 1986).

The excellent agreement between simulation and DDM results across both output metrics validates the model's accuracy for comprehensive uncertainty quantification analysis. This confirmation enables reliable use of the data-driven approach for further system investigations without requiring additional computationally intensive simulations.

3. Results and discussion

3.1. UQ analysis

Fig. 7 presents the Pearson correlation heatmap analysing relationships between input parameters and system outputs in the hybrid ammonia production system (Üstün et al., 2024). The heatmap evaluates correlations between six uncertain inputs - heat exchanger effectiveness values HE1 through HE4, power input Pin, and compressor efficiency ($C_{\rm eff}$), and two key outputs: ammonia production (NH₃) and refrigeration generation (Ref). The diagonal elements naturally display perfect correlation coefficients of one, representing each parameter's correlation with itself.

The analysis reveals statistically significant positive correlations between power input Pin and both system outputs, with p-values of 0.009 for ammonia production and 0.007 for refrigeration generation, underscoring Pin's critical influence on system performance. Among the heat exchangers, HE1 and HE4 show meaningful correlations with outputs (p = 0.016–0.038), confirming their substantial contribution to heat recovery efficiency. In contrast, HE2, HE3 and compressor efficiency $C_{\rm eff}$ demonstrate weaker correlations (p > 0.1) with both NH3 and Ref production, indicating their relatively minor impact under the examined operating conditions. These quantitative insights help identify

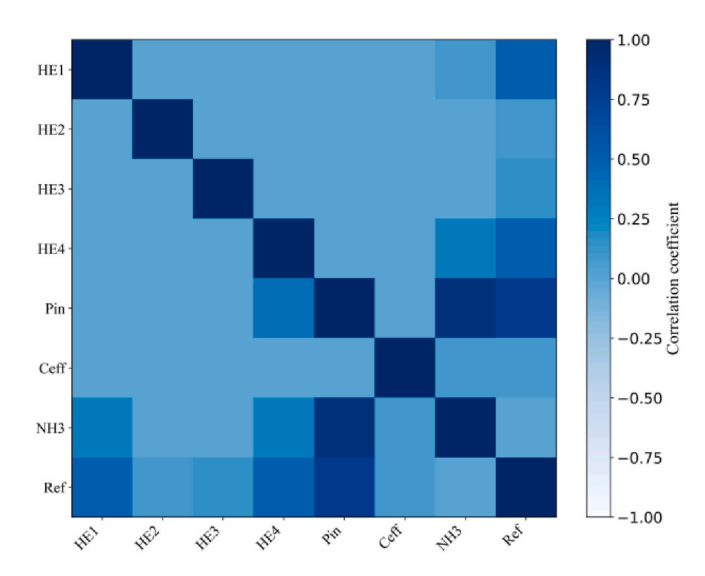


Fig. 7. Heatmap of Pearson correlation between the input and output parameters.

the most influential parameters for system optimisation while highlighting components where performance improvements would yield limited benefits.

The correlation patterns align with the system's thermodynamic behaviour, where power input and primary heat exchangers dominate the energy conversion processes, while secondary heat exchangers and compression efficiency play more peripheral roles in overall performance. These findings provide valuable guidance for prioritising operational monitoring and maintenance efforts in the hybrid ammonia production system.

More results are produced by using UQTk to generate the combination of input parameters and data driven model was used to generate results with respect to that specific combination of parameters. Fig. 8 shows the PDFs of different scaled HB sub-system for ammonia production and refrigeration from hybridised HB and vapour absorption refrigeration cycle. Fig. 8a presents the uniformly distributed curve of the minimum and maximum values of ammonia production, along with the system's PDF across the 10 MW–20 MW range. In contrast, Fig. 8b illustrates the minimum and maximum values of refrigeration generation from hybridised ammonia production system for nominal power inputs (10 MW–20 MW), where the PDF follows a bell-shaped (normal) distribution. The difference in probability density function shapes between Fig. 8a and b is driven by the distinct uncertainty propagation mechanisms in ammonia and refrigeration production. Ammonia production followed a uniform distribution, suggesting that input

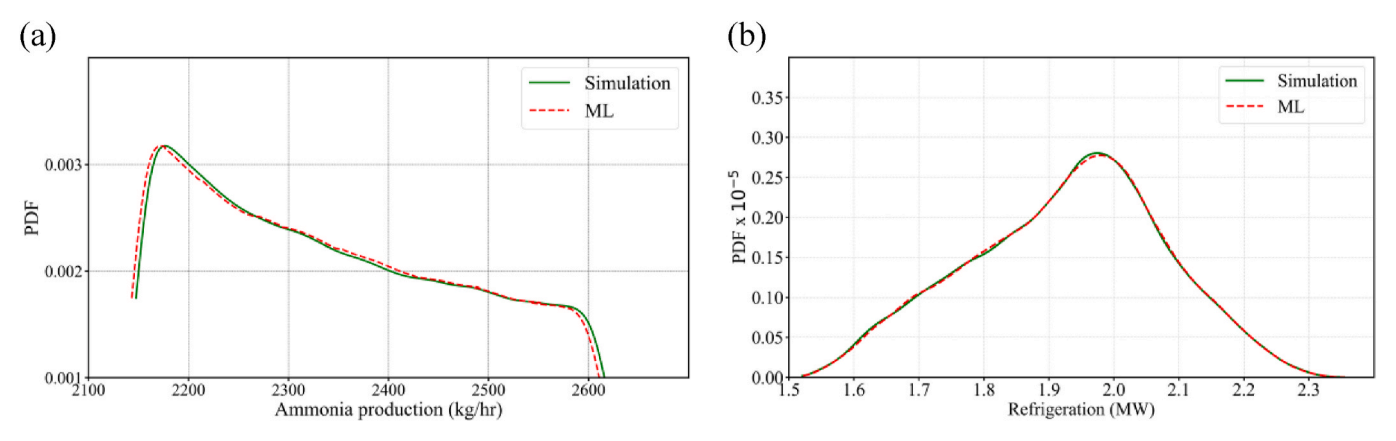


Fig. 6. Validation of ML model, comparison of the ML and simulations-based PDFs of (a) ammonia production, (b) refrigeration.

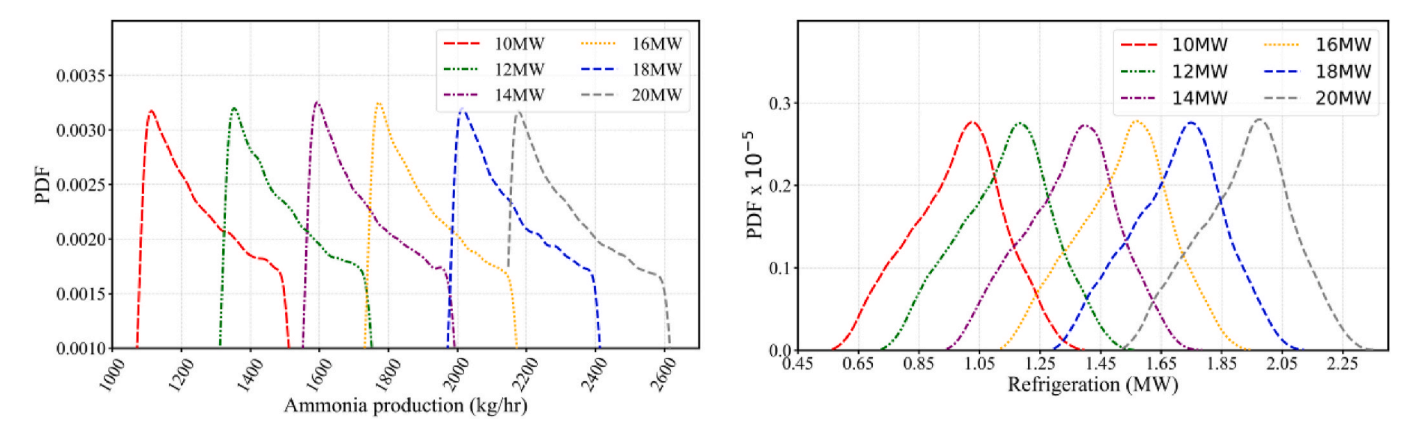


Fig. 8. PDFs of the hybridised ammonia production system for different values of the nominal power input of (a) ammonia production, (b) refrigeration.

uncertainties were evenly distributed, leading to a uniform spread of output values. In contrast, refrigeration production exhibits a normal distribution due to the nonlinear interactions of uncertain parameters introduced by the VARC in hybridised ammonia production system. The combined effects of uncertainties, resulting in a bell-shaped distribution where values concentrate around a mean. This distinction underscores the differing stochastic behaviour of ammonia and refrigeration production in the hybridised system.

Fig. 9 shows the effect of uncertainty in input parameters (showed in Table 1) on ammonia production and refrigeration generation from hybridised ammonia production system. Fig. 9a shows the variation in the ammonia production due to the uncertainties in HB sub-systems for nominal power inputs. Overall, approximately 18 % variability in the ammonia production is noticed due to the uncertainty in the performance of heat exchangers, compressors, and input power. Similarly, Fig. 9b shows the variation in the refrigeration production due to the uncertainties in hybridised ammonia production systems for nominal power inputs. Uncertainty in the performance of heat exchangers, compressors, and power input led to a 30 % variation in refrigeration production by the VARC system when coupled with the HB sub-system. This significant variation is expected due to the VARC system's heavy reliance on heat exchangers. A reduction in heat exchanger effectiveness can directly cause up to a 30 % decline in VARC output. In contrast, the smaller variation observed in ammonia production is due to the HB subsystem being less dependent on heat exchanger performance compared to VARC system.

Fig. 10 presents the sensitivity analysis of uncertainties in 10–20 MW HB sub-systems and hybridised ammonia production systems. Fig. 10a

illustrates the sensitivity of uncertain components affecting ammonia production in the HB sub-system, while Fig. 10b highlights the impact of component performance uncertainties on refrigeration generation within the hybridised ammonia production system.

In both cases—ammonia production and refrigeration—the most sensitive variable is the power supply ($P_{\rm in}$) which is almost 50 % in case with Fig. 10a and more than 50 % if we look at Fig. 10b. This is due to its role as the primary energy supplier of the whole hybridised system. Another significant source of uncertainty is the effectiveness of heat exchangers which is within 12 %–18 % range. HE1 is responsible for cooling the gas mixture to 350 °C before it enters the HB reactor. In the hybridised system, this heat exchanger also functions as a preheater when integrated with VARC. Consequently, any uncertainty in its effectiveness affects the output of both systems.

HE2 and HE3 represent uncertainties in the effectiveness of the heat exchangers used to cool the hydrogen and oxygen streams exiting the water electrolyser. Since these streams have moderate temperatures (70–90 $^{\circ}$ C), variations in their effectiveness have minimal impact (less than 5 %) on ammonia production. However, in the hybridised ammonia production system for refrigeration, these heat exchangers serve as preheaters in the VARC, meaning their performance uncertainty directly influences system output (5 %–10 %). HE4 is the heat exchanger responsible for cooling the gas mixture downstream of the HB reactor to separate ammonia from the unreacted mixture. In the hybridised system, this heat exchanger also connects the HB sub-system to VARC. Therefore, any inefficiency in HE4 due to performance uncertainty has a more pronounced impact on the overall system (23 %–33 %). Additionally, $C_{\rm eff}$ represents the impact of uncertainty in the compressor's

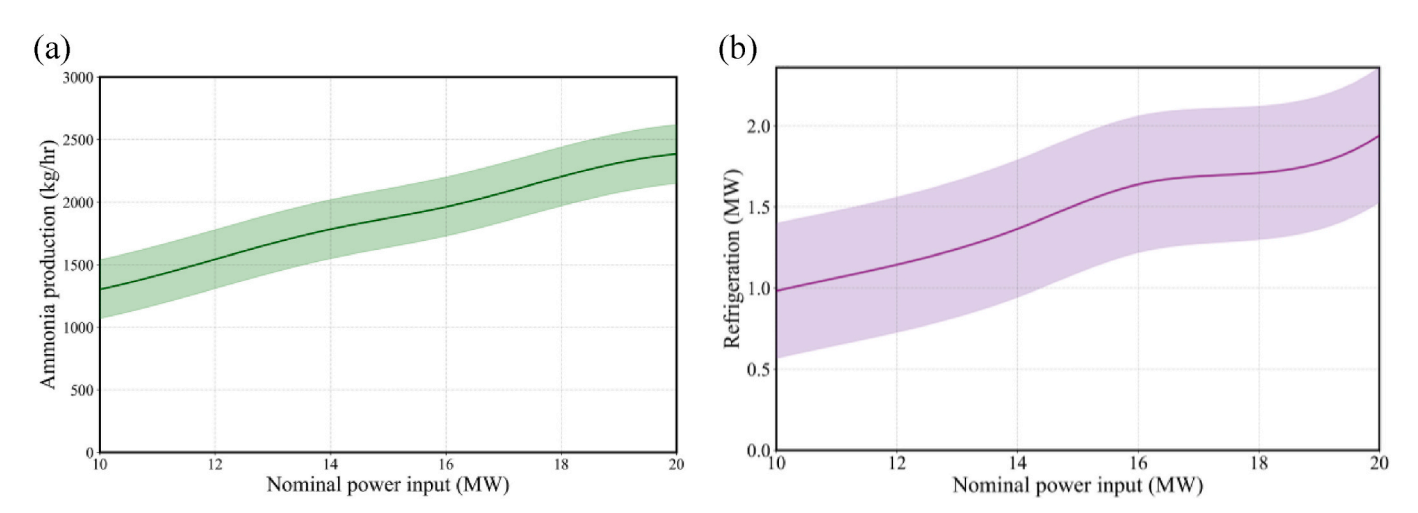


Fig. 9. Effects of input parameters variability on (a) ammonia production, (b) refrigeration generation.

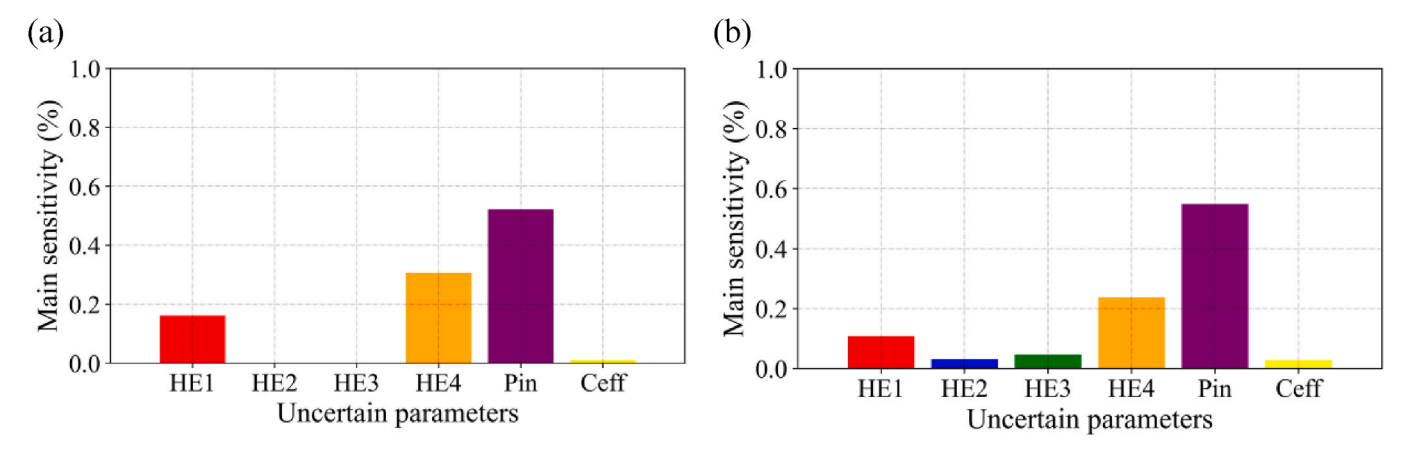


Fig. 10. Main sensitivity of all uncertain parameters in (a) HB sub-system, (b) hybridised ammonia production system.

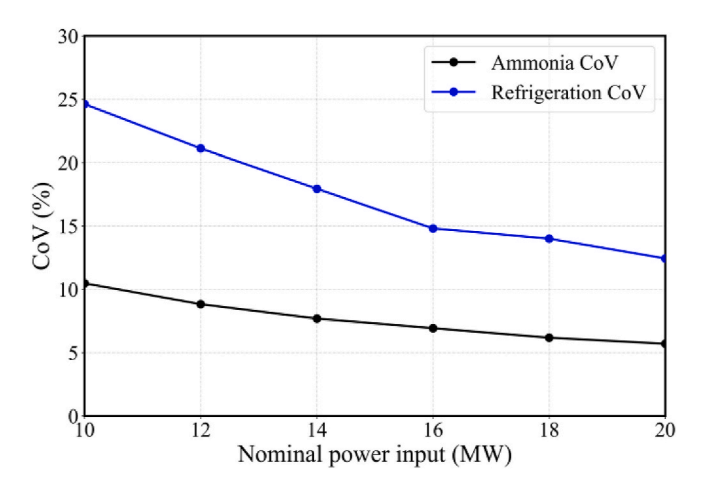


Fig. 11. Coefficient of variance of the hybridised ammonia production system for different values of the nominal power input.

isentropic efficiency, further influencing system performance.

Fig. 11 presents the coefficient of variance (see (Brown, 1998) for definition) of ammonia production from HB sub-system and refrigeration generation from the hybridised ammonia production system. The trend of CoV for both ammonia production and refrigeration generation are similar. It can be seen that as the capacity of HB sub-system increases, the values of CoV converges towards a reasonable range for complex engineering systems, i.e. 15-20 % (Shechtman, 2013). Overall, for both HB sub-system for ammonia production and hybridised ammonia production system for refrigeration generation, the data for CoV are in acceptable ranges. It can be noticed that as the capacity of the system increases the CoV becomes more stable. This behaviour might be because as the system capacity increases, the production of ammonia and refrigeration increases significantly, which increases the mean value and the corresponding uncertainties does not increase to the same extend, lowering the impact of uncertainties.

For better understanding, an analysis is conducted to observe the impact of individual uncertainties in the system on ammonia production and refrigeration generation. Fig. 12 shows the range of variation in ammonia production due to the uncertainties in performance of the components of HB sub-system. Fig. 12a shows the range in variation in the ammonia production which is around 50 %. This is due to the uncertain power input because of intermittent power supply from renewable energy sources. Fig. 12b and c presents the variation range in ammonia production due to the uncertainties in the effectiveness of heat exchangers (HE1, HE4). The effectiveness of heat exchangers is the cause of the remaining 50 % of the overall uncertainty in the system.

Fig. 12d shows the range in variation in output due to the uncertainty in compressor efficiencies (C_{eff}) over time. Clearly, the most significant impact on output is due to the uncertainty in power input. In contrast, the variations in the output caused due to the uncertainty in the effectiveness of heat exchangers are comparatively much smaller. Nevertheless, both combined could lead to up to 50 % of the overall uncertainties in the HB sub-system.

Similarly, Fig. 13 shows the variation range in ammonia production due to the uncertainties in hybridised ammonia production system for nominal power inputs. Fig. 13a shows the variation range in the output due to the uncertainty in the power supply, which could be significant due to the intermittent supply of renewable power. Fig. 13b shows the variation range in refrigeration generation due to the uncertainty in heat exchanger (HE1) which is one of the three preheaters in VARC and extract waste heat from HB sub-system.

Figs. 13c and 12d present the variation range in refrigeration caused by the uncertainties in the effectiveness of heat exchangers. These two heat exchangers (HE2, HE3), which are the other two preheaters in VARC are transferring waste heat from water electrolyser hydrogen and oxygen outlet streams. It can be noticed the variation range (2 %–4 %) is not significant as the heat extraction from water electrolyser streams is relatively small (Anwar et al., 2024). Fig. 13e illustrates the range of variations in refrigeration output caused by uncertainty in the effectiveness of the heat exchanger (HE4), which connects the HB sub-system to the VARC. As the primary component of WHR in the hybridised ammonia production system, this heat exchanger plays a crucial role in transferring thermal energy to the VARC. Any uncertainty in its effectiveness has a significant impact, potentially leading to fluctuations exceeding 20 % in refrigeration generation.

Fig. 13f presents the variations in system output resulting from uncertainties in compressor efficiencies ($C_{\rm eff}$). Overall, the results indicate that uncertainty in power input has the most substantial influence on system performance. Additionally, variations in heat exchanger effectiveness contribute significantly, accounting for approximately 50 % of the total uncertainties in the hybridised ammonia production system.

3.2. Environmental and economic analysis

The environmental analysis adopted U.S. energy sector assumptions from the EIA (EIA, 2022), where electricity generation is sourced from natural gas (40 %), coal (20 %), nuclear (18 %), and renewables (22 %). This mix results in substantial GHG emissions: $80 \% CO_2$ (0.85 kg/kWh), $11 \% CH_4$ (0.015 kg/kWh), and $6.1 \% N_2O$ (0.001 kg/kWh). The assessment assumed that conventional vapour compression refrigeration requires 284.33 W of electric power per kilowatt of cooling (EIA, 2022). By integrating a renewable-powered HB process with a VARC, the system recovers waste heat to provide cooling, thereby reducing emissions—although the extent of reduction is influenced by system

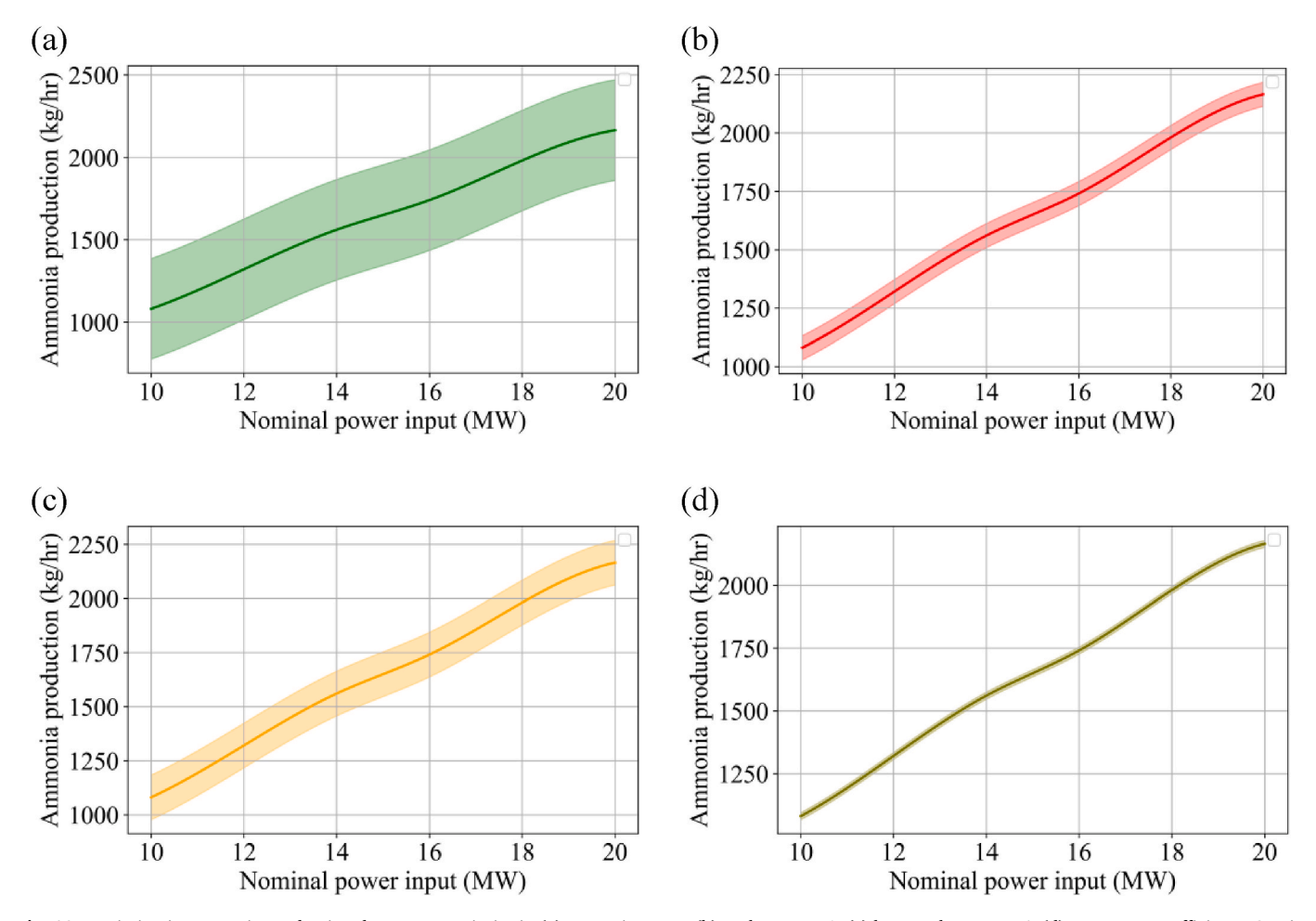


Fig. 12. Variation in ammonia production due to uncertainties in (a) power input P_{in} (b) preheater HE1, (c) heat exchanger HE4, (d) compressors efficiency C_{eff} , in the HB sub-system for different values of the nominal power input.

uncertainties. The VARC's cooling output replaces that which would otherwise be generated by electricity-intensive vapour compression systems, serving as a low-carbon energy vector since it is derived from renewable sources rather than fossil fuels.

For a 20 MW HB system hybridised with VARC, refrigeration generation reaches approximately 2.163 MW (204.8 tonnes of refrigeration), displacing conventional electricity needs estimated at 0.721 MW (assuming a COP of 3). Fig. 14 demonstrates that system uncertainties create significant variations in environmental benefits - up to 30 % fluctuation in refrigeration output and 40–50 % variation in GHG reductions. Since the refrigeration cycle directly offsets conventional energy demand, any output reduction proportionally increases grid/fossil fuel dependence, elevating emissions. This sensitivity highlights refrigeration stability's critical role in maximising carbon credits and minimising environmental impact (Chen et al., 2022; Woo et al., 2021), emphasising the need to address uncertainties for optimising the system's sustainability performance.

It should be noted that the current environmental assessment focuses on avoided operational carbon emissions under uncertainty. Embodied carbon from infrastructure and system components is assumed fixed and excluded, so the results reflect changes in emission reduction potential due to operational variability rather than the total lifecycle footprint.

In Fig. 15, the overview of the variation in the annual revenue due to the uncertainties in hybridised ammonia production systems for nominal power inputs is illustrated. The calculations and discussions of LCOA and the associated CAPEX and OPEX were reported in a recent study (Anwar et al., 2024). The LCOA for the HB sub-system was determined to be 0.65 \$/kg, aligning well with the literature-reported range of

0.58–1.2 \$/kg (Nayak-Luke et al., 2018a). It was established from the previous study that the LCOA of HB sub-system remains practically neutral when integrated with VARC, this is due to the reason that the extra installation overheads of VARC were balanced from the savings achieved through the produced refrigeration. The following Eq. (8) presents the equation for LCOA estimation (Nayak-Luke et al., 2018b; Osman et al., 2020).

$$LCOA = \frac{\sum_{t=1}^{n} \frac{I_{t} + M_{t} + E_{t}}{(1+r)^{t}}}{\sum_{t=1}^{n} \frac{G_{t}}{(1+r)^{t}}}$$
(8)

where ' I_t ' represents the capital cost, ' M_t ' denotes the operation or maintenance cost, 'Et' is the utility cost which is the cost of electricity in the current scenario and was assumed to be \$0.03/kWh (EIA, 2022), 'Gt' represents the production generation, 't' is the project life span, "r' shows the discount rate, which is 8 %, 'n' here is the number of years, which was assumed to be 10 years and cost of ammonia was assumed to be \$0.61/kg (EIA, 2022; Liu et al., 2024).

However, this claim has been made without the consideration of uncertainties in the system. Considering those uncertainties, 30– $40\,\%$ of the variation in the annual revenue generation from refrigeration is observed. Accounting the uncertainties, the value of LCOA increased from $0.65\,$ \$/kg to $0.68\,$ \$/kg, escalated by $5\,\%$, highlighting the economic impact of variability. The 30– $40\,\%$ fluctuation in annual refrigeration revenue underscores the need to account the uncertainty quantification to ensure the economic viability of integrated ammonia production.

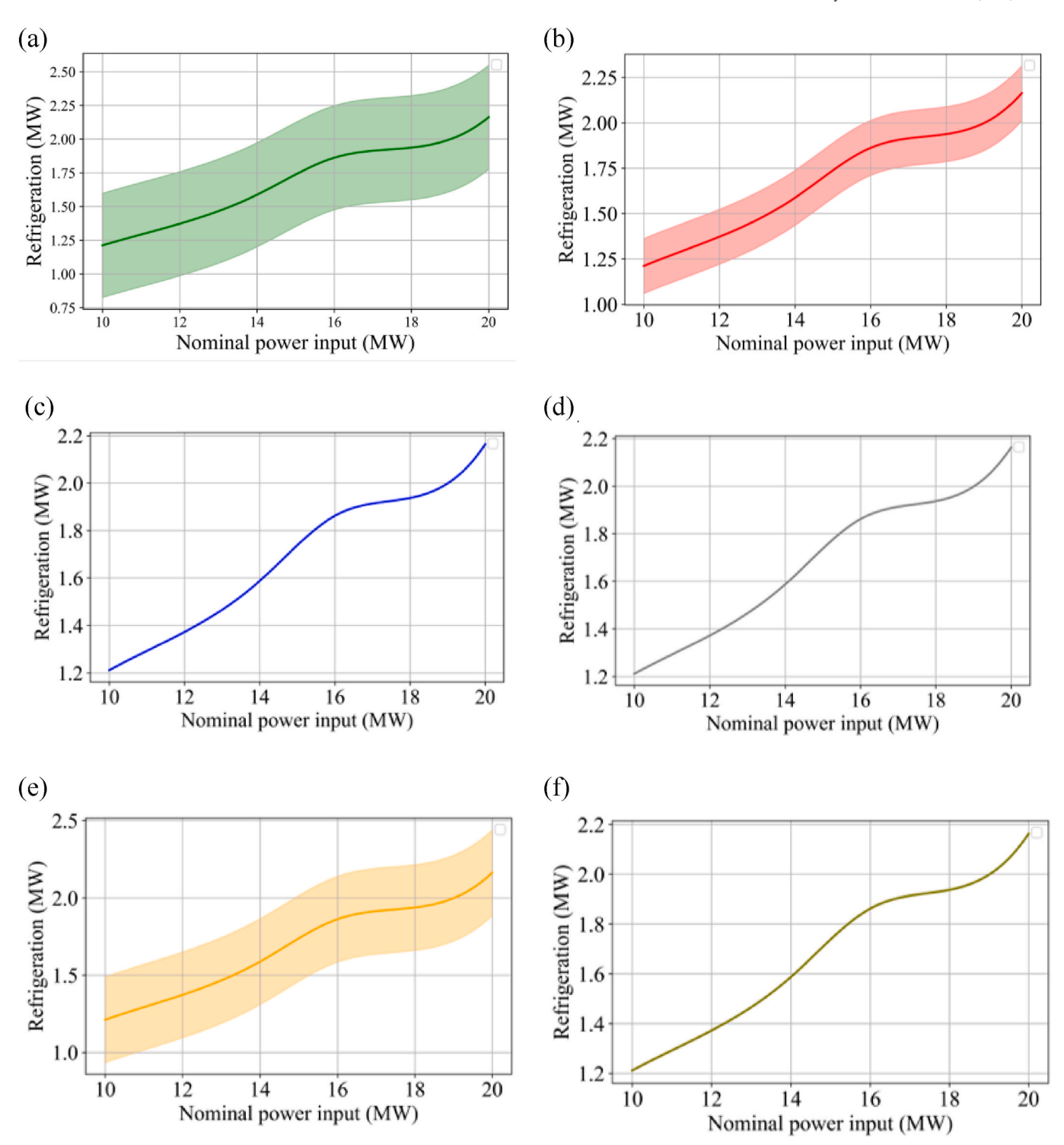


Fig. 13. Variation in refrigeration generation due to uncertainties in (a) power input P_{in} (b) preheater HE1, (c) preheater HE2, (d) preheater HE3, (e) heat exchanger HE4, (f) compressors efficiency C_{eff} , in the hybridised ammonia production system for different values of the nominal power input.

4. Conclusions

This study introduced a robust machine learning—enhanced uncertainty quantification (ML-UQ) framework to evaluate the technoeconomic and environmental performance of a hybrid ammonia production system powered by renewable energy. High-fidelity Aspen Plus simulations were performed across six nominal power inputs (10–20 MW) to generate a dataset for training a feedforward artificial neural network (ANN) with autoregressive feedback. The ANN surrogate

accurately captured the complex nonlinear interactions among six key uncertain parameters—renewable power input, four heat exchanger effectiveness values, and compressor efficiency—and critical outputs, including ammonia production and refrigeration capacity. Statistical metrics confirmed its predictive fidelity: $R^2=0.97$, MAE = 8.57, RMSE = 11.3, and Grayson Index = 0.98, validating its use for subsequent uncertainty propagation via polynomial chaos expansion. UQ analysis revealed strong sensitivity of system outputs to parameter uncertainties: ammonia production varied by up to 18 %, refrigeration output by 30 %,

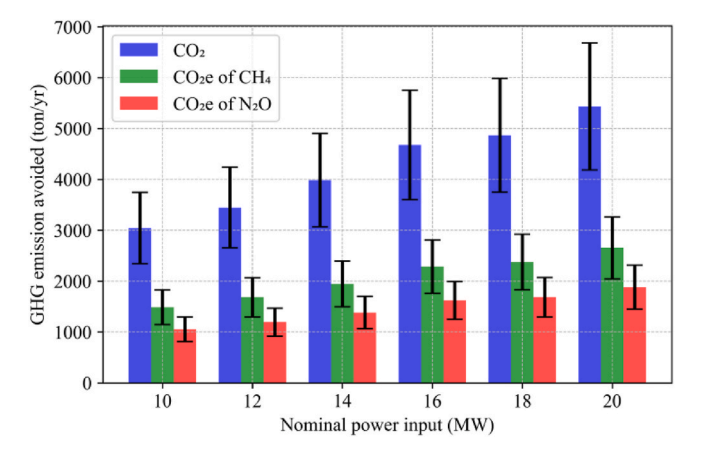


Fig. 14. Variation in GHG emission avoided due to uncertainties in hybridised ammonia production system for different values of the nominal power input.

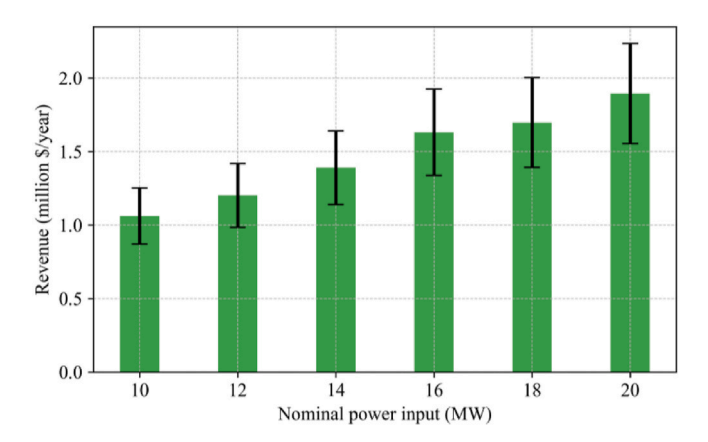


Fig. 15. Variation in revenue generation due to uncertainties in the hybridised ammonia production system for different values of nominal power input.

and CO2 emissions reduction potential by 40-50 %. Heat exchanger effectiveness emerged as the dominant contributor, accounting for nearly 50 % of total variability. Economically, uncertainties led to a modest 5 % increase in the levelized cost of ammonia, with 30-40 % variability in annual refrigeration revenue. The ML-UQ methodology enabled a scalable and computationally efficient assessment of nonlinear system behaviour under uncertainty, reducing computational cost by three orders of magnitude while maintaining high predictive accuracy. This efficiency facilitates analysis of complex, large-scale systems and provides critical insights into the resilience and reliability of renewable-integrated ammonia processes under quasi-steady-state conditions. While the study assumed independent, uniformly distributed uncertainties and did not capture short-term dynamics, it lays a foundation for future work incorporating unsteady-state effects, temporal dynamics, and correlated or non-uniform inputs to more closely reflect real-world operations. Overall, this work advances surrogateassisted UO and demonstrates the value of combining machine learning with process modelling for the optimisation of next-generation sustainable energy technologies. The proposed framework is generalisable and practical, offering an effective approach for uncertaintyaware decision-making in complex energy and manufacturing systems.

CRediT authorship contribution statement

Muzumil Anwar: Writing – review & editing, Writing – original draft, Validation, Software, Methodology, Investigation, Formal analysis, Data curation. **Israfil Soyler:** Writing – review & editing, Software, Methodology. **Nader Karimi:** Writing – review & editing, Supervision,

Project administration, Conceptualization.

Declaration of competing interest

The authors declare that they have no known competing financial interests or personal relationships that could have appeared to influence the work reported in this paper.

Acknowledgement

Muzumil Anwar acknowledges the support of the Higher Education Commission (HEC), Ministry of Education, Pakistan for PhD scholarship. N. Karimi acknowledges the financial support provided by EPSRC through grant number EP/X019551/1.

During the preparation of this work the authors used Chat GPT in order to improve the clarity of text in some parts of the manuscript. After using this service, the authors reviewed and edited the content as needed and take full responsibility for the content of the publication.

Data availability

Data will be made available on request.

References

Abdar, M., Pourpanah, F., Hussain, S., Rezazadegan, D., Liu, L., Ghavamzadeh, M., Fieguth, P., Cao, X., Khosravi, A., Acharya, U.R., 2021. A review of uncertainty quantification in deep learning: techniques, applications and challenges. Inf. Fusion 76. 243–297.

Adeli, K., Nachtane, M., Tarfaoui, M., Faik, A., Pollet, B., Saifaoui, D., 2024. Deep learning analysis of green ammonia synthesis: evaluating techno-economic feasibility for sustainable production. Int. J. Hydrogen Energy 87, 1224–1232.

Almodfer, R., Zayed, M.E., Abd Elaziz, M., Aboelmaaref, M.M., Mudhsh, M., Elsheikh, A. H., 2022. Modeling of a solar-powered thermoelectric air-conditioning system using a random vector functional link network integrated with jellyfish search algorithm. Case Stud. Therm. Eng. 31, 101797.

Anwar, M., Mehdizadeh, A., Karimi, N., 2024. Waste heat recovery from a green ammonia production plant by Kalina and vapour absorption refrigeration cycles: a comparative energy, exergy, environmental and economic analysis. Sustain. Energy Technol. Assessments 69, 103916.

Bert Debusschere, C.C., Safta, Cosmin, Johnston, Katherine, Chowdhary, Kenny, 2024. UQ toolkit. UQ Toolkit version 3.1.1. https://www.sandia.gov/uqtoolkit/.

Bilionis, I., Zabaras, N., 2012. Multi-output local Gaussian process regression: applications to uncertainty quantification. J. Comput. Phys. 231 (17), 5718–5746.

Brown, C.E., 1998. Coefficient of variation. In: Brown, C.E. (Ed.), Applied Multivariate Statistics in Geohydrology and Related Sciences. Springer Berlin Heidelberg, pp. 155–157. https://doi.org/10.1007/978-3-642-80328-4_13.

Chen, Z., Zhang, Y., Wang, H., Ouyang, X., Xie, Y., 2022. Can green credit policy promote low-carbon technology innovation? J. Clean. Prod. 359, 132061.

Chitransh, A., Bindal, R.K., 2021. A review on energy storage system of smart grid system. Int. J. Sci. Res. 10 (6). published in.

Davidson, J., 1994. Stochastic Limit Theory: an Introduction for Econometricians. OUP, Oxford.

Deng, Z., Zhang, L., Miao, B., Liu, Q., Pan, Z., Zhang, W., Ding, O.L., Chan, S.H., 2024. A novel combination of machine learning and intelligent optimization algorithm for modeling and optimization of green ammonia synthesis. Energy Convers. Manag. 311, 118429.

Díaz-Motta, A., Díaz-González, F., Villa-Arrieta, M., 2023. Energy sustainability assessment of offshore wind-powered ammonia. J. Clean. Prod. 420, 138419. https://doi.org/10.1016/j.jclepro.2023.138419.

Egolfopoulos, F.N., Hansen, N., Ju, Y., Kohse-Höinghaus, K., Law, C.K., Qi, F., 2014. Advances and challenges in laminar flame experiments and implications for combustion chemistry. Prog. Energy Combust. Sci. 43, 36–67.

EIA, 2022. U.S. Energy information administration (EIA). https://www.eia.gov/.
El-Maghraby, R.M., Mohamed, A.Y., Hassanean, M., 2024. Improving energy efficiency in ammonia production plants using machine learning. Fuel 363, 130910.

Frattini, D., Cinti, G., Bidini, G., Desideri, U., Cioffi, R., Jannelli, E., 2016. A system approach in energy evaluation of different renewable energies sources integration in ammonia production plants. Renew. Energy 99, 472–482.

Gholaminezhad, I., Assimi, H., Jamali, A., Vajari, D.A., 2016. Uncertainty quantification and robust modeling of selective laser melting process using stochastic multiobjective approach. Int. J. Adv. Des. Manuf. Technol. 86, 1425–1441.

Gillcrist, D.J., Alemazkoor, N., Chen, Y., Tootkaboni, M., 2024. Design of experiments via multi-fidelity surrogates and statistical sensitivity measures. J. Mach. Learn. for Model. Comput. 5 (4).

Gresh, T., 2018. Compressor Performance: Aerodynamics for the User. Butterworth-Heinemann.

- Helton, J.C., Johnson, J.D., Oberkampf, W.L., Sallaberry, C.J., 2010. Representation of analysis results involving aleatory and epistemic uncertainty. Int. J. Gen. Syst. 39 (6), 605–646.
- Indyk, P., Motwani, R., 1998. Approximate nearest neighbors: towards removing the curse of dimensionality. In: Proceedings of the thirtieth annual ACM symposium on Theory of computing.
- Ishaq, H., Dincer, I., 2020. Design and simulation of a new cascaded ammonia synthesis system driven by renewables. Sustain. Energy Technol. Assessments 40, 100725.
- Jain, V., Kachhwaha, S., Sachdeva, G., 2013. Thermodynamic performance analysis of a vapor compression–absorption cascaded refrigeration system. Energy Convers. Manag. 75, 685–700.
- Jansohn, P., 2013. Modern Gas Turbine Systems: High Efficiency, Low Emission, Fuel Flexible Power Generation.
- Karimi Shoar, Z., Pourpasha, H., Zeinali Heris, S., Mousavi, S.B., Mohammadpourfard, M., 2023. The effect of heat transfer characteristics of macromolecule fouling on heat exchanger surface: a dynamic simulation study. Can. J. Chem. Eng. 101 (10), 5802–5817.
- Klaas, L., Guban, D., Roeb, M., Sattler, C., 2021. Recent progress towards solar energy integration into low-pressure green ammonia production technologies. Int. J. Hydrogen Energy 46 (49), 25121–25136.
- Knio, O.M., Najm, H.N., Ghanem, R.G., 2001. A stochastic projection method for fluid flow: I. Basic formulation. J. Comput. Phys. 173 (2), 481–511.
- Kucherenko, S., Song, S., 2017. Different numerical estimators for main effect global sensitivity indices. Reliab. Eng. Syst. Saf. 165, 222–238.
- Laimon, M., Goh, S., 2024. Unlocking potential in renewable energy curtailment for green ammonia production. Int. J. Hydrogen Energy 71, 964–971.
- Le Mattre, O.P., Reagan, M.T., Najm, H.N., Ghanem, R.G., Knio, O.M., 2002. A stochastic projection method for fluid flow: II. Random process. J. Comput. Phys. 181 (1), 9-44
- Lee, B., Heo, J., Choi, N.H., Moon, C., Moon, S., Lim, H., 2017. Economic evaluation with uncertainty analysis using a Monte-Carlo simulation method for hydrogen production from high pressure PEM water electrolysis in Korea. Int. J. Hydrogen Energy 42 (39), 24612–24619.
- Lee, Y.-J., Kang, J.-K., Jung, S.-H., Lee, C.-G., Park, S.-J., Park, J.-M., Park, C., 2024. Prediction and optimization of the efficiency and energy consumption of an ammonia vacuum thermal stripping process using experiments and machine learning models. Environ. Technol. Innov. 34, 103610.
- Liu, F., Moustafa, H., He, Z., 2024. Simultaneous recovery of nitrogen and phosphorus from actual digester centrate in an electrochemical membrane system. Resour. Conserv. Recycl. 203, 107463. https://doi.org/10.1016/j.resconrec.2024.107463.
- Lou, F., Fabian, J., Key, N.L., 2013. The effect of gas models on compressor efficiency including uncertainty. J. Eng. Gas Turbines Power 136 (1). https://doi.org/10.1115/ 1.4025317.
- Mueller, J.N., Sargsyan, K., Daniels, C.J., Najm, H.N., 2025. Polynomial Chaos surrogate construction for random fields with parametric uncertainty. SIAM/ASA J. Uncertain. Quantification 13 (1), 1–29.
- Najm, H.N., 2009. Uncertainty quantification and polynomial chaos techniques in computational fluid dynamics. Annu. Rev. Fluid Mech. 41 (1), 35–52.
- Najm, H.N., Debusschere, B.J., Marzouk, Y.M., Widmer, S., Le Maître, O., 2009. Uncertainty quantification in chemical systems. Int. J. Numer. Methods Eng. 80 (6-7), 789–814.
- Nami, H., Hendriksen, P.V., Frandsen, H.L., 2024. Green ammonia production using current and emerging electrolysis technologies. Renew. Sustain. Energy Rev. 199, 114517.
- Nannapaneni, S., Mahadevan, S., 2014. Uncertainty Quantification in Performance Evaluation of Manufacturing Processes. 2014 IEEE International Conference on Big Data (Big Data).
- Nayak-Luke, R., Bañares-Alcántara, R., Wilkinson, I., 2018a. "Green" ammonia: impact of renewable energy intermittency on plant sizing and levelized cost of ammonia. Ind. Eng. Chem. Res. 57 (43), 14607–14616. https://doi.org/10.1021/acs. iecr.8b02447.
- Nayak-Luke, R., Bañares-Alcántara, R., Wilkinson, I., 2018b. "Green" ammonia: impact of renewable energy intermittency on plant sizing and levelized cost of ammonia. Ind. Eng. Chem. Res. 57 (43), 14607–14616.
- Osman, O., Sgouridis, S., Sleptchenko, A., 2020. Scaling the production of renewable ammonia: a techno-economic optimization applied in regions with high insolation. J. Clean. Prod. 271, 121627.
- Palmer, K.A., Hale, W.T., Such, K.D., Shea, B.R., Bollas, G.M., 2016. Optimal design of tests for heat exchanger fouling identification. Appl. Therm. Eng. 95, 382–393.
- Park, J., Gbadago, D.Q., Mori, S., Hwang, S., 2025. Renewable ammonia synthesis via experiments and optimization using periodic operation and machine learning integrated approaches. Energy Convers. Manag. 324, 119286.
- Qaiyum, S., Irshad, K., Zayed, M.E., Algarni, S., Alqahtani, T., Khan, A.I., 2025. Benchmarking reinforcement learning and accurate modeling of ground source heat pump systems: intelligent strategy using spiking recurrent neural network combined with spider wasp inspired optimization Algorithm. Results Eng., 105724
- Rajeh, T., Al-Kbodi, B.H., Li, Y., Zhao, J., Zayed, M.E., Rehman, S., 2024. Comparative numerical modeling complemented with multi-objective optimization and dynamic life cycle assessment of coaxial ground heat exchangers with oval-shaped and typical circular-shaped configurations. Appl. Therm. Eng. 244, 122673.
- Reagan, M.T., Najm, H.N., Pébay, P.P., Knio, O.M., Ghanem, R.G., 2005. Quantifying uncertainty in chemical systems modeling. Int. J. Chem. Kinet. 37 (6), 368–382.
- Rehman, S., Zayed, M.E., Irshad, K., Menesy, A.S., Kotb, K.M., Alzahrani, A.S., Alhems, L. M., 2024. Design, commissioning and operation of a large-scale solar linear Fresnel system integrated with evacuated compound receiver: field testing, thermodynamic

- analysis, and enhanced machine learning-based optimization. Sol. Energy 278, 112785
- Samitha Weerakoon, A.H., Assadi, M., 2024. Techno economic analysis and performance based ranking of 3–200 kW fuel flexible micro gas turbines running on 100% hydrogen, hydrogen fuel blends, and natural gas. J. Clean. Prod. 477, 143819. https://doi.org/10.1016/j.jclepro.2024.143819.
- Sanchez, M., Amores, E., Abad, D., Rodriguez, L., Clemente-Jul, C., 2020. Aspen plus model of an alkaline electrolysis system for hydrogen production. Int. J. Hydrogen Energy 45 (7), 3916–3929.
- Sargsyan, K., Safta, C., Boll, L., Johnston, K., Khalil, M., Chowdhary, K., Rai, P., Casey, T., Zeng, X., Debusschere, B., 2022. Uqtk Version 3.1. 2 User Manual.
- Sarker, I.H., 2021. Machine learning: Algorithms, real-world applications and research directions. SN comput. sci. 2 (3), 160.
- Shamsi, M., Karami, B., Cheraghdar, A., Mousavian, S., Makki, M., Rooeentan, S., 2024. Evaluation of an environmentally-friendly poly-generation system driven by geothermal energy for green ammonia production. Fuel 365, 131037.
- Shechtman, O., 2013. The coefficient of variation as an index of measurement reliability. Methods Clin. Epidemiol. 39–49. https://doi.org/10.1007/978-3-642-37131-8 4.
- Smith, R.C., 2024. Uncertainty Quantification: Theory, Implementation, and Applications. SIAM.
- Snoek, J., Larochelle, H., Adams, R.P., 2012. Practical bayesian optimization of machine learning algorithms. Adv. Neural Inf. Process. Syst. 25.
- Soyler, I., Zhang, K., Duwig, C., Jiang, X., Karimi, N., 2023. Uncertainty quantification of the premixed combustion characteristics of NH3/H2/N2 fuel blends. Int. J. Hydrogen Energy 48 (38), 14477–14491. https://doi.org/10.1016/j. ijhydene.2022.12.303.
- Soyler, I., Zhang, K., Jiang, X., Karimi, N., 2024. Effects of compositional uncertainties in cracked NH3/biosyngas fuel blends on the combustion characteristics and performance of a combined-cycle gas turbine: a numerical thermokinetic study. Int. J. Hydrogen Energy 69, 504–517.
- Spanos, A., 1986. Statistical Foundations of Econometric Modelling. Cambridge University Press.
- Suberu, M.Y., Mustafa, M.W., Bashir, N., 2014. Energy storage systems for renewable energy power sector integration and mitigation of intermittency. Renew. Sustain. Energy Rev. 35, 499–514.
- Tripathy, R., Bilionis, I., Gonzalez, M., 2016. Gaussian processes with built-in dimensionality reduction: applications to high-dimensional uncertainty propagation. J. Comput. Phys. 321, 191–223.
- Üstün, C.E., Eckart, S., Valera-Medina, A., Paykani, A., 2024. Data-driven prediction of laminar burning velocity for ternary ammonia/hydrogen/methane/air premixed flames. Fuel 368, 131581.
- Verleysen, K., Coppitters, D., Parente, A., De Paepe, W., Contino, F., 2020. How can power-to-ammonia be robust? Optimization of an ammonia synthesis plant powered by a wind turbine considering operational uncertainties. Fuel 266, 117049.
- Wang, H., 2019. Uncertainty quantification and minimization. In: Computer Aided Chemical Engineering, vol. 45. Elsevier, pp. 723–762.
- Wang, Y., Wang, Z., Sheng, H., 2024. Optimizing wind turbine integration in microgrids through enhanced multi-control of energy storage and micro-resources for enhanced stability. J. Clean. Prod. 444, 140965. https://doi.org/10.1016/j. iclepro.2024.140965.
- Wang, Z., Dahl, G.E., Swersky, K., Lee, C., Nado, Z., Gilmer, J., Snoek, J., Ghahramani, Z., 2024. Pre-trained Gaussian processes for Bayesian optimization. J. Mach. Learn. Res. 25 (212) 1–83
- Woo, J., Fatima, R., Kibert, C.J., Newman, R.E., Tian, Y., Srinivasan, R.S., 2021. Applying blockchain technology for building energy performance measurement, reporting, and verification (MRV) and the carbon credit market: a review of the literature. Build. Environ. 205, 108199. https://doi.org/10.1016/j.buildenv.2021.108199.
- Xing, Z., Jiang, X., 2024. Neural network potential-based molecular investigation of pollutant formation of ammonia and ammonia-hydrogen combustion. Chem. Eng. J. 489, 151492. https://doi.org/10.1016/j.cej.2024.151492.
- Xiong, F., Chen, S., Xiong, Y., 2014. Dynamic system uncertainty propagation using polynomial chaos. Chin. J. Aeronaut. 27 (5), 1156–1170.
- Xiu, D., Karniadakis, G.E., 2002. The Wiener–Askey polynomial chaos for stochastic differential equations. SIAM J. Sci. Comput. 24 (2), 619–644.
- Yang, B., Chen, Y., Guo, Z., Wang, J., Zeng, C., Li, D., Shu, H., Shan, J., Fu, T., Zhang, X., 2021. Levenberg-Marquardt backpropagation algorithm for parameter identification of solid oxide fuel cells. Int. J. Energy Res. 45 (12), 17903–17923.
- Yin, N., 2024. Enhancing energy efficiency and reducing emissions in a novel biomass-geothermal hybrid system for hydrogen/ammonia production using machine learning and multi-level heat recovery. Int. J. Hydrogen Energy 92, 959–974.
- Yuen, C., Oudalov, A., Timbus, A., 2010. The provision of frequency control reserves from multiple microgrids. IEEE Trans. Ind. Electron. 58 (1), 173–183.
- Zaki, A.M., Zayed, M.E., Alhems, L.M., 2024. Leveraging machine learning techniques and in-situ measurements for precise predicting the energy performance of regenerative counter-flow indirect evaporative cooler in a semi-arid climate building. J. Build. Eng. 95, 110318.
- Zayed, M.E., Kabeel, A., Shboul, B., Ashraf, W.M., Ghazy, M., Irshad, K., Rehman, S., Zayed, A.A., 2023. Performance augmentation and machine learning-based modeling of wavy corrugated solar air collector embedded with thermal energy storage: support vector machine combined with Monte Carlo simulation. J. Energy Storage 74, 109533.
- Zayed, M.E., Rehman, S., Elgendy, I.A., Al-Shaikhi, A., Mohandes, M.A., Irshad, K., Abdelrazik, A., Alam, M.A., 2025. Benchmarking reinforcement learning and prototyping development of floating solar power system: experimental study and LSTM modeling combined with brown-bear optimization algorithm. Energy Convers. Manag. 332, 119696.

- Zhang, K., Jiang, X., 2018. An investigation of fuel variability effect on bio-syngas
- combustion using uncertainty quantification. Fuel 220, 283–295.
 Zhang, T., Uratani, J., Huang, Y., Xu, L., Griffiths, S., Ding, Y., 2023. Hydrogen liquefaction and storage: recent progress and perspectives. Renew. Sustain. Energy Rev. 176, 113204. https://doi.org/10.1016/j.rser.2023.113204.
- Zhang, Y., Peng, X., Yuan, X., Li, Y., Wang, K., 2023. A unidirectional cascaded highpower wind converter with reduced number of active devices. IEEE Access 11, 10902–10911.
- Zubair, S.M., Sheikh, A.K., Younas, M., Budair, M., 2000. A risk based heat exchanger analysis subject to fouling: part I: performance evaluation. Energy 25 (5), 427–443.